NEOPLASIA
www.neoplasia.com

Volume 10 Number 8 August 2008 pp. 886–896 886

Thrombospondin 1 and Vasoactive Agents Indirectly Alter Tumor Blood Flow[1,2]

Jeff S. Isenberg*, Fuminori Hyodo†, Lisa A. Ridnour†, Caitlin S. Shannon*, David A. Wink†, Murali C. Krishna† and David D. Roberts*

*Laboratory of Pathology, Center for Cancer Research, National Cancer Institute, National Institutes of Health, Bethesda, MD 20892, USA; †Radiation Biology Branch, Center for Cancer Research, National Cancer Institute, National Institutes of Health, Bethesda, MD 20892, USA

Abstract

Nitric oxide (NO) plays important physiological roles in the vasculature to regulate angiogenesis, blood flow, and hemostasis. In solid tumors, NO is generally acknowledged to mediate angiogenic responses to several growth factors. This contrasts with conflicting evidence that NO can acutely increase tumor perfusion through local vasodilation or diminish perfusion by preferential relaxation of peripheral vascular beds outside the tumor. Because thrombospondin 1 (TSP1) is an important physiological antagonist of NO in vascular cells, we examined whether, in addition to inhibiting tumor angiogenesis, TSP1 can acutely regulate tumor blood flow. We assessed this activity of TSP1 in the context of perfusion responses to NO as a vasodilator and epinephrine as a vasoconstrictor. Nitric oxide treatment of wild type and TSP1 null mice decreased perfusion of a syngeneic melanoma, whereas epinephrine transiently increased tumor perfusion. Acute vasoactive responses were also independent of the level of tumor-expressed TSP1 in a melanoma xenograft, but recovery of basal perfusion was modulated by TSP1 expression. In contrast, overexpression of truncated TSP1 lacking part of its CD47 binding domain lacked this modulating activity. These data indicate that TSP1 primarily regulates long-term vascular responses in tumors, in part, because the tumor vasculature has a limited capacity to acutely respond to vasoactive agents.

Neoplasia (2008) 10, 886–896

Introduction

Solid tumor growth requires the generation of new blood vessels from an established vascular network, a process termed *angiogenesis*. The newly formed vascular network provides necessary nutrients and oxygen to meet the increased metabolic demand of the growing tumor. Tumor angiogenesis is an intensely pursued therapeutic target for treating cancers. Although several antiangiogenic drugs have attained US Food and Drug Administration approval and significantly delay tumor progression, hypertension is a frequent adverse effect of these agents [1]. If arteries supplying the tumor are selectively constricted, this adverse effect could contribute to the efficacy of antiangiogenic drugs. If instead these drugs induce systemic hypertension, the resulting increased tumor perfusion could limit their efficacy [2,3].

Although long-term control of angiogenesis can clearly limit tumor growth, acute regulation of tumor blood flow and dynamics may be more difficult. The intratumor vasculature is poorly organized, and it displays variability in flow and tissue perfusion. Intratumoral vessels typically lack anatomic elements required for normal vasoactive responses including autonomic neural elements [4]. Additionally, some

Abbreviations: BAEC, bovine aortic endothelial cell; BOLD, blood oxygen level–dependent; DEA/NO, diethylamine NONOate; DETA/NO, diethyltriamine NONOate; MSME, multislice multiecho; sGC, soluble guanylyl cyclase; TSP1, thrombospondin 1; VSMC, vascular smooth muscle cell

Address all correspondence to: David D. Roberts, National Institutes of Health, Building 10, Room 2A33, 10 Center Dr MSC1500, Bethesda, MD, 20892.
E-mail: droberts@helix.nih.gov

[1]This research was supported by the Intramural Research Program of the National Institutes of Health, National Cancer Institute, Center for Cancer Research (D.D.R., M.C.K., and D.A.W.).

[2]This article refers to the supplementary materials, which are designated by Movies W1–W3 and are available online at www.neoplasia.com.

Received 5 February 2008; Revised 20 May 2008; Accepted 21 May 2008

Copyright © 2008 Neoplasia Press, Inc. All rights reserved 1522-8002/08/$25.00
DOI 10.1593/neo.08264

tumors lack lymphatic vessels, which combined with increased vascular permeability increases interstitial pressure and decreases tumor perfusion [5]. Increased tumor interstitial pressure encourages vascular and lymphatic collapse, stagnation, and reversal of arterial flow [5,6]. Consequently, tumor blood flow is very heterogeneous, with areas of significant under perfusion and hypoxia [7]. Additionally, tumor vessels display dynamic changes that are specific for the growth stage of the tumor [8]. Such irregularity in flow confounds effective delivery of therapeutic agents to tumor tissue [9,10]. In contrast, adjacent blood vessels that feed tumor vessels do contain normal vascular anatomy and should respond to vasoactive challenges in a predictable fashion. Limiting tumor perfusion with agents that can predictably enhance or retard tumor blood flow represents a potential therapeutic avenue [11,12]. An alternative strategy to acutely control flow using agents that cause rapid tumor vascular thrombosis and obliteration has also shown promise [13].

Nitric oxide (NO) is an important signaling molecule for acute regulation of blood flow and for long-term angiogenic responses. It is constantly produced by vascular cells, and it relaxes the arterial component of blood vessels [14]. The direct effect of vessel relaxation is to increase blood flow and tissue perfusion. Chronic exposure to NO drives the formation of new blood vessels by stimulating both endothelial and vascular smooth muscle cell (VSMC) proliferation and migration as part of a physiologic response to normal wound healing and during tumor growth and metastasis [15,16]. Furthermore, endogenous NO can be limiting for tumor blood flow [17]. Several studies have reported that inhibition of NO synthase using either *N*-nitro-L-arginine methyl ester or N^{ω}-nitro-L-arginine results in decreased total tumor blood flow in animal models [18–22] or has inhibitory effects on tumor growth [23]. These reports are supported by studies demonstrating that tumor blood flow is increased by exogenous NO donors [24] (and reviewed in Refs. [25–27]). Other studies, however, found that NO can decrease tumor blood flow in animal models, which has been attributed to a steal effect [28].

Consistent with these conflicting studies in rodents, attempts to demonstrate therapeutic responses through manipulation of tumor blood flow have been modest in people [23,29–31]. Nonspecific inhibition of endogenous NO production in a recent phase I trial in patients with several tumor types documented immediate decreases in tumor blood volume using contrast-enhanced computed tomography [30]. In some cases, tumor blood volume remained decreased for 24 hours. In contrast, treatment of patients with hepatic tumors using a continuous infusion of epinephrine increased tumor blood flow in 66% of cases [32].

The matricellular protein thrombospondin 1 (TSP1) was the first identified endogenous angiogenesis inhibitor [33,34]. Its expression is frequently lost in some types of human tumors. Conversely, overexpression of TSP1 in experimental tumors dramatically decreases tumor growth rate, neovascularization, and metastasis [35]. Thrombospondin 1 inhibits NO signaling in both endothelial and VSMC by inhibiting activation of soluble guanylyl cyclase (sGC) [15,36]. In VSMC and *in vivo*, TSP1 limits vasorelaxation by NO [37]. Under an ischemic stress, blocking TSP1 acutely increases tissue blood flow and perfusion [37]. The ability of TSP1 to abrogate NO-stimulated angiogenesis and blood flow changes requires the cell surface receptor CD47 [36]. Targeting this receptor mimics the inhibitory actions of TSP1 on NO-driven vascular responses [38].

Given the pivotal role that TSP1 plays in controlling NO-driven vascular responses and blood flow in nontumor vascular networks, we hypothesized that, in addition to its antiangiogenic activity, TSP1 may acutely regulate flow in the peritumoral or tumoral vasculature. A recent histochemical analysis of pancreatic tumors in mice treated with recombinant TSP1 type 1 repeats inferred that this treatment decreased tumor blood flow [39], but a direct assessment of flow was not performed. Here, we approach this question by assessing the role of host and tumor TSP1 expression in regulating acute tumor blood flow responses. We present evidence that vasoactive agents such as NO and epinephrine primarily alter tumor perfusion in an indirect manner. Thrombospondin 1 expressed in the tumor vasculature does not alter such blood flow responses to vasoactive stimuli. In contrast, overexpression of TSP1 by tumor cells moderately decreases tumor blood flow responses to NO and epinephrine. These results provide important insights for evaluating efforts to directly alter tumor blood flow using vasoactive agents and for maximizing the efficacy of angiogenesis inhibitors.

Materials and Methods

Animals

Wild type and TSP1 null C57BL/6 mice were housed in a pathogen-free environment and had *ad libitum* access to standard rat chow and water. Cr(Cnr)athymic<nu>fBf female mice were obtained from Charles River (Taconic, MD). Care and handling of animals comply with standards established by the Animal Care and Use Committee of the National Cancer Institute.

Reagents and Cells

The murine B16F10 melanoma cell line was kindly provided by Dr. Lyuba Varticovski. Cells were expanded in standard growth medium (RPMI with 10% FCS; Gibco, Grand Island, NY) and frozen at uniform passage for injection in mice. The human melanoma cell line, MDA-MB-435, was previously transfected with a CMV-*THBS1* expression plasmid, and TSP1 expression was quantified as described [40]. The parental cell line, a TSP1-overexpressing clone (TH26) and a clone expressing a C-terminal truncation of TSP1 (TH50) were used. Cells were MAP tested and expanded in complete DMEM containing 10% fetal bovine serum and 750 μg/ml G418 (Gibco-BRL, Gaithersburg, MD) and frozen for future use. Porcine femoral artery VSMC were harvested from Yucatan white hairless miniature pigs and cultured in SM-GM +2.5% FCS (Lonza, Belgium). Bovine aortic endothelial cells (BAECs) were prepared from fresh aortic segments and grown in DMEM containing 10% fetal bovine serum, penicillin G (100 units/ml), and streptomycin (100 μg/ml).

Blood Oxygen Level–Dependent Magnetic Resonance Imaging

Magnetic resonance imaging (MRI) scans were acquired using a 4.7-T scanner (Bruker BioSpin, Karlsruhe, Germany) and isoflurane anesthesia. Muscle and tumor tissue was scanned at rest, so alterations in oxygenation reflected changes in perfusion rather than in oxygen consumption. Magnetic resonance measurements were started after the mouse's body temperature reached 37°C. Before the experiments, a multislice multiecho (MSME) sequence was used to determine the target slice location. A series of T_2*-weighted gradient echo blood oxygenation level–dependent (BOLD) image data sets transverse to the midpoint of the femur were repeatedly acquired

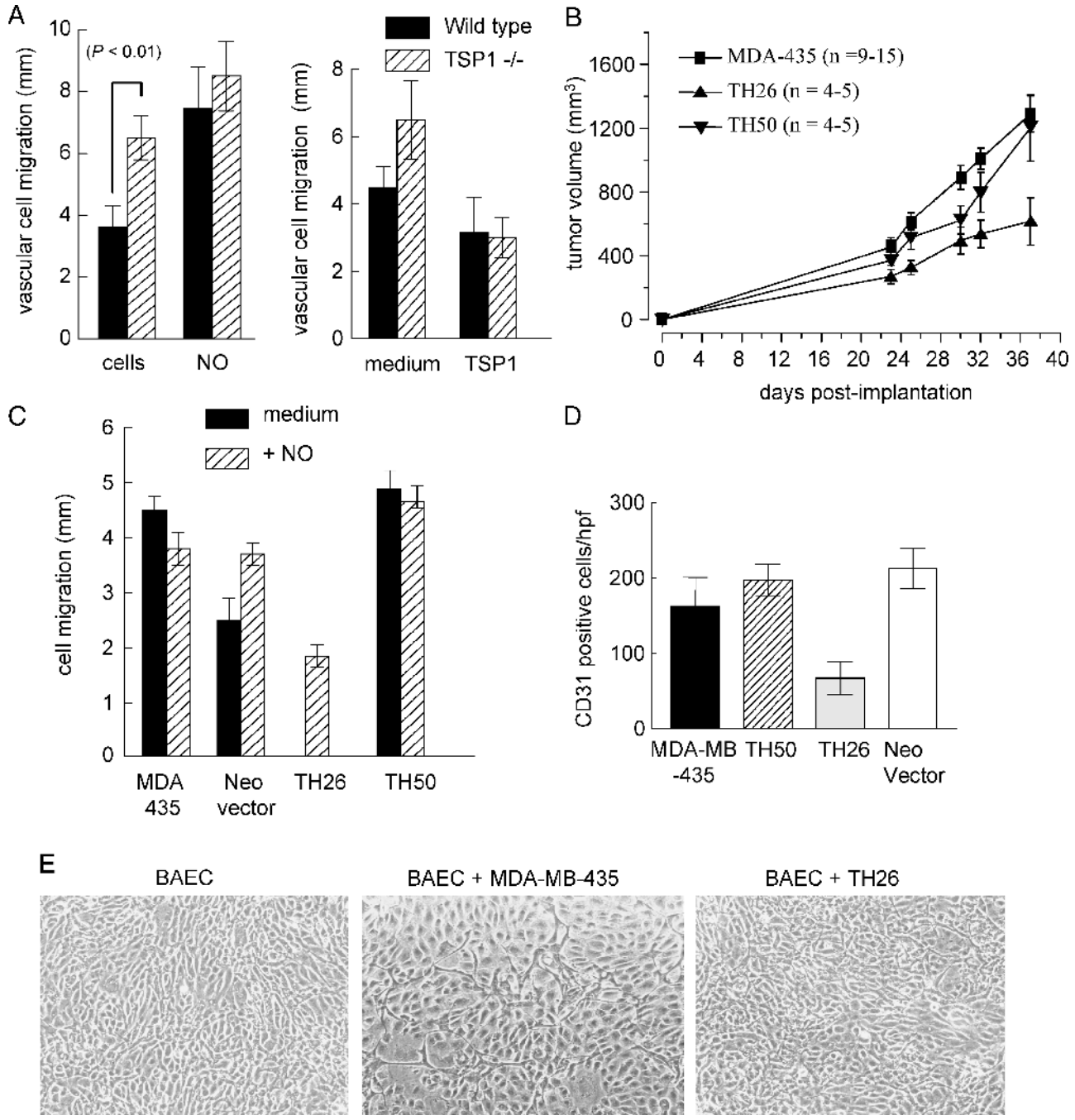

Figure 1. NO-stimulated angiogenesis in B16F10 melanomas is inhibited by exogenous TSP1. B16F10 tumor biopsies (1 mm^3) excised from sex- and age-matched wild type and TSP1 null mice were embedded in three-dimensional collagen matrix and incubated in growth medium ± DETA/NO (10 μM) (A, left panel) or ± TSP1 (2.2 nM; A, right panel). Sex- and age-matched athymic nude mice were injected with equal numbers of control MDA-MB-435, clone TH26, or clone TH50 tumor cells to the lateral thigh. Tumor size was determined with calipers by the same examiner at the indicated time intervals, and volumes were calculated (B). Sex- and age-matched athymic nude mice were injected with equal numbers of MDA-MB-435, Neo vector-transfected, clone TH26, or clone TH50 cells to the lateral thigh. Equal sized tumors were excised, and 1 mm^3 biopsies were embedded in collagen matrix with growth medium ± NO (DETA/NO 10 μM) (C). After 7 days of incubation, vascular cell invasion was quantified as the distance of farthest cell invasion from the biopsy border in each of four quadrants. Sex- and age-matched athymic nude mice were injected with equal numbers of MDA-MB-435, Neo vector-transfected, clone TH26, or clone TH50 cells to the lateral thigh. Equal sized tumors were excised, and 1-mm^3 biopsies were embedded in collagen matrix with growth medium. After 7 days of incubation, cytospin immunocytochemistry of matrix-invading cells was performed. CD31-positive staining cells were counted in 10 random high-power fields from each tumor explant and presented as mean ± SD (D). Bovine aortic endothelial cells were cultured under empty Transwell chambers or chambers that contained parental MDA-MB-435 or clone TH26 cells, and the BAECs were imaged (E). Results are representative of three independent experiments.

for 30 minutes to monitor temporal changes in blood oxygenation and blood flow. Diethylamine NONOate (DEA/NO; 100 nmol/g body weight) was injected with normal saline through rectal cannula 5.0 minutes after starting the scan. Imaging parameters used were as follows: T_R, 450 milliseconds; flip angle, 45°; number of excitations, 2; slice thickness, 2 mm; matrix size, 64 × 64; number of scans, 30; total imaging time for the series, 29 minutes.

Laser Doppler Analysis of Tumor and Hindlimb Perfusion

Cr(Cnr)athymic<nu>fBf nude female mice 8 weeks in age were injected subcutaneously with 10^6 tumor cells to the lateral thigh. Doppler analysis of tumor perfusion was performed when tumors reached 1 cm^3 in size. Core temperature was monitored through rectal probe and maintained precisely at 35°C by a heated stage and heat lamp. Anesthesia was obtained with 1.5% isoflurane. Under loop magnification, the cutaneous envelope over each tumor was carefully excised, protecting the vascular network decorating the tumor mass. A MoorLD1-2λ scanner (Moor Instruments, Devon, UK) was used with the following parameters: scan area, 1.6 × 2.5 cm; scan speed, 4 msec/pixel; scan time, 1 minutes 54 seconds; override distance, 20 cm. After obtaining baseline tumor perfusion data, animals received either 0.05 μg of epinephrine i.p. in sterile warmed saline or 1 μl/g body weight of a 100-mM stock solution of DEA/NO. Tumor perfusion was then measured. Perfusion was also determined in normal hind limbs in sex-, age-, and weight-matched C57BL/6 or athymic mice after DEA/NO administration (1 μl/g weight of a 100-mM stock) using the same anesthetic/physiologic parameters and imaging conditions.

Intracellular cGMP Assay

Cells were plated at a density 1 × 10^6 cells/well in 12-well culture plates (Nunc) in standard medium and weaned over 48 hours of serum and treated in basal medium + 0.1% BSA with the indicated agents. Total cGMP was determined through immunoassay (Amersham, GE Healthcare, UK). In some experiments, equal numbers of MDA-MB-435, clone TH26, and clone TH50 cells were plated in six-well plates in standard growth medium and were allowed to adhere for 6 hours; medium was replaced with serum-free RPMI with 0.1% BSA. Cells were incubated for 12 hours overnight; conditioned medium was collected, diluted at the indicated concentrations in fresh serum-free RPMI with 0.1% BSA, applied ± DEA/NO to porcine VSMC; and cGMP was determined.

Tumor Growth Studies

To confirm growth rates of the cancer cell lines, separate cohorts of 8-week-old female Cr(Cnr)athymic<nu>fBf mice were injected subcutaneously with 10^6 tumor cells to the lateral thigh. Tumor growth was measured by the same investigator at twice weekly intervals.

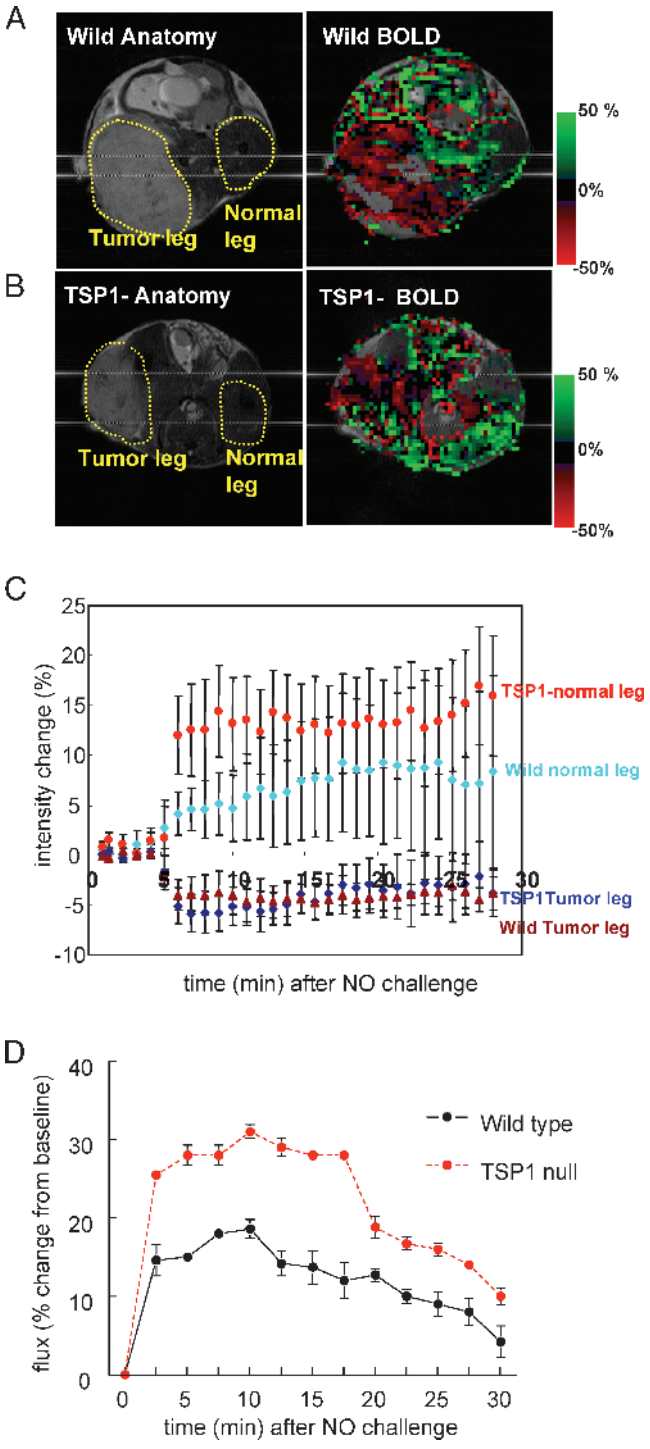

Figure 2. Differential BOLD response and effect of TSP1 in tumor and normal leg. Anatomic and BOLD MR scans for (A) WT and (B) TSP1 null mice bearing B16F10 melanoma tumors 1000 mm^2 in size were obtained from T_2*-weighted MSME sequences. DEA/NO (100 nmol/g body weight) was injected with saline through an intrarectal cannula 5 minutes after starting the scan. Green and red colors show positive and negative BOLD MRI signals, respectively, at the indicated times after NO administration. The BOLD images were superimposed with the corresponding anatomic images to determine exact locations in the lateral thigh sections. Averaged BOLD MRI signal changes (C) in tumor and normal leg as a function of time after NO challenge. The green and red plots show increased and decreased BOLD MRI signals, respectively. Values are presented as mean ± SE from five and six experiments in WT and TSP1 null mice, respectively. Age- and sex-matched C57BL/6 wild type and TSP1 null mice underwent laser Doppler analysis of normal hind limbs (D). After obtaining baseline perfusion data, DEA/NO (1 μl/g weight of 100-mM stock) was given through rectal bolus. Data sampling was then done every 2.5 minutes. Results represent the mean ± SD of four separate animals of each strain.

Tumor volume was calculated by the formula: volume = $W^2 \times L/2$, where W = shortest diameter and L = longest diameter. For each cell line, six mice per group were used.

Tumor Explant Assay

Tumor biopsies that had reached 1 cm^3 were harvested from WT, TSP1 null, and Cr(Cnr)athymic<nu>fBf nude mice and were explanted in type I collagen as described [15]. Explants were incubated in the presence of DMEM with FCS and the indicated treatment agents for 7 days, and cell migration through the extracellular matrix was measured. Results represent the mean ± SD of at least three separate experiments.

Immunohistochemistry

Tumor explants were prepared as described. On postexplantation day 7, tumor biopsies were removed from the constructs, and the collagen gel was digested with type II collagenase (Worthington, Lakewood, NJ). The mixture was centrifuged, supernatant was aspirated, and cells were resuspended in basal medium without serum. Cells were attached to charged glass slides (Fisherbrand Superfrost Slides; Fischer Scientific, Pittsburgh, PA) by cytospinning at 1000 rpm for 5 minutes and then fixed and rehydrated through 80%, 70%, and 50% alcohol. Slides were rinsed with PBS and then incubated with 3% H_2O_2 for 30 minutes at room temperature. Sections were then blocked with 100% normal goat serum in PBS for 30 minutes at room temperature, washed, and incubated 1 hour with a rat antimouse monoclonal CD31 antibody (clone MEC 13.3; BD Pharmingen, Franklin Lakes, NJ) at 1:100 dilution. Slides were washed and incubated with a rat antimouse IgG secondary antibody (ALX-211-052; Alexis Biochemicals, San Diego, CA) diluted at 1:5000 for 45 minutes, washed with PBS, and incubated in prediluted streptavidin–HRP conjugate (BD Pharmingen) for 45 minutes at room temperature. Color was developed by DAB substrate kit (BD Pharmingen). Slides were counterstained using Mayer's hematoxylin for 2 minutes, dehydrated, and mounted. CD31-positive cells were counted in 10 randomly selected high-power fields for each tumor explant type.

Endothelial and Tumor Cell Coculture Experiments

Bovine aortic endothelial cells (4×10^4 cells/well) were plated in 24-well culture plates in DMEM + 10% FCS and allowed to reach confluence. MDA-MB-435 cells or TSP1-transfected MDA-MB-435 cells (clone TH-26, 5000 cells/well) were plated onto Transwell inserts (Falcon, Becton Dickinson, NJ) in RPMI 1640 medium and allowed to adhere. Inserts were then placed in wells containing BAEC and incubated for 1 week in DMEM at 37°C and 5% CO_2. Bovine aortic endothelial cells were then fixed with 1% glutaraldehyde, and images were acquired in phase-contrast illumination with a microscope (Model IX 70; Olympus, Center Valley, PA).

Statistics

All experiments were replicated at least three times. Results are presented as mean ± SD with analysis of significance using Student's *t* test or one-way or two-way analysis of variance (ANOVA) with Tukey's *post hoc* test where indicated using Origin software (version 7; OriginLab Corp., Northampton, MA), with significance taken at P values < .05.

Results

Vascular and Tumor-Derived TSP1 Limit Tumor Angiogenic Responses

Expression of TSP1 either by tumor cells or by the host is known to limit melanoma tumor growth in mice [40,41]. To assess whether tumor and host TSP1 differentially regulate NO-stimulated tumor angiogenic responses, we used a previously published *ex vivo* assay that quantifies vascular outgrowth and invasion through a three-dimensional type I collagen matrix [42]. Explants from B16F10 melanomas grown in wild type and TSP1 null animals were embedded into three-dimensional type I collagen matrices, and vascular cell invasion and migration through the matrix were quantified (Figure 1*A*). Vascular outgrowth was consistently greater in melanoma explants from TSP1 null animals. Treating with a slow-releasing NO-donor diethyltriamine NONOate (DETA/NO) enhanced the vascular cell

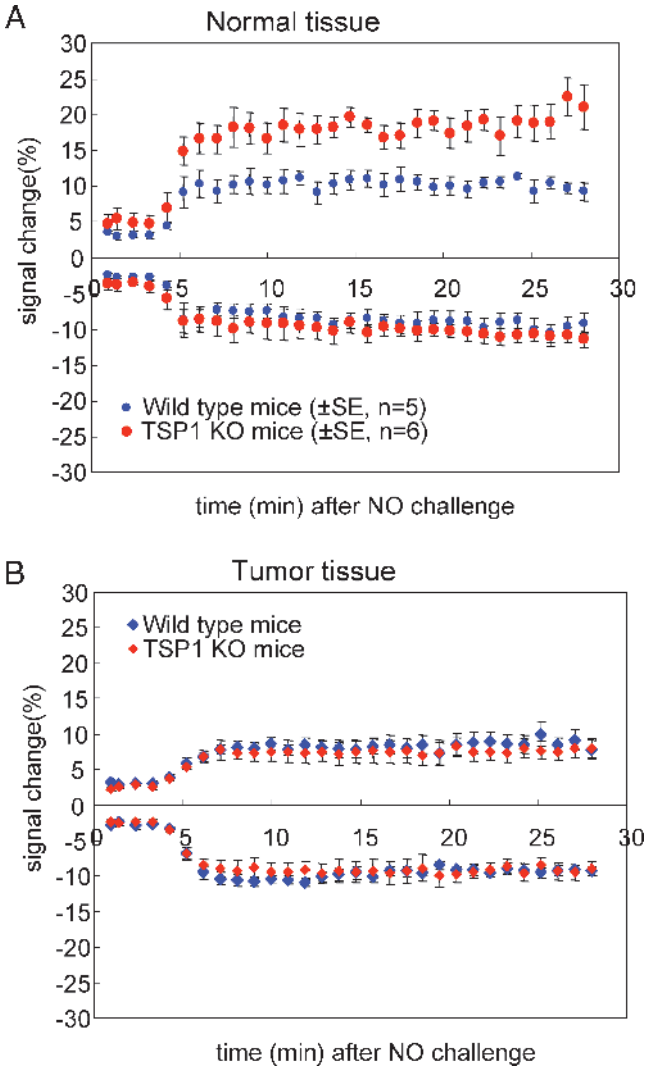

Figure 3. Differential BOLD response and effect of TSP1 in tumor and normal leg. Blood oxygen level–dependent MR scans for WT and TSP1 null mice bearing B16F10 melanoma tumors 1000 mm^2 in size were obtained from T_2*-weighted MSME sequences. Positive (A) and negative (B) BOLD MRI signal changes are presented in tumor and normal leg as a function of time after NO challenge.

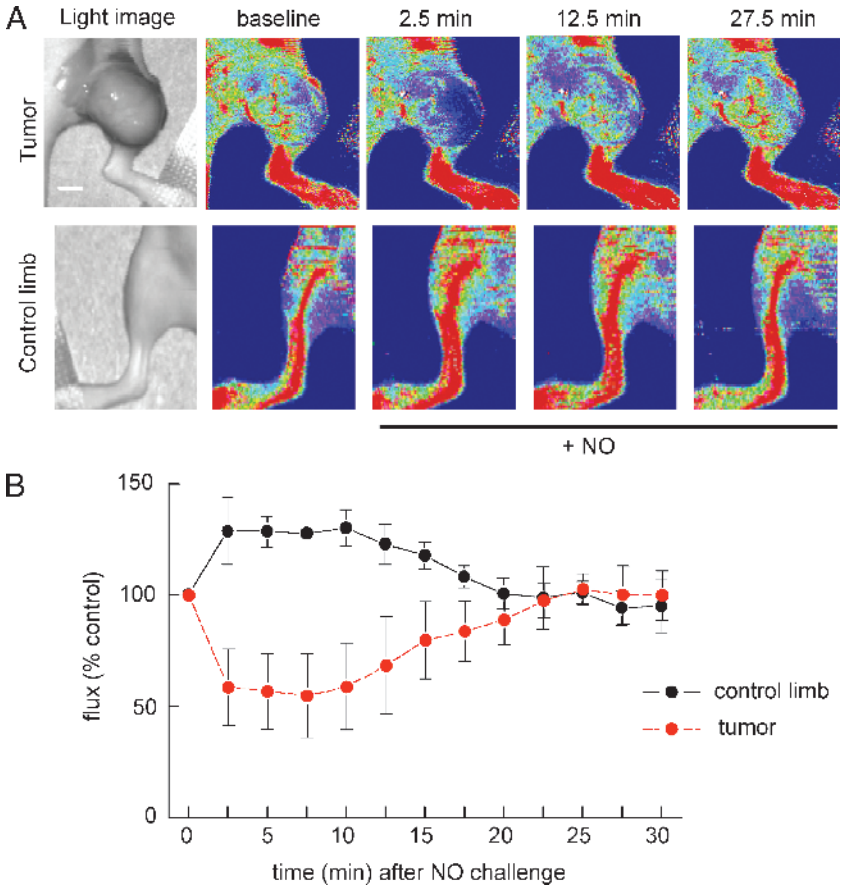

Figure 4. Nitric oxide challenge simultaneously decreases MDA-435 tumor blood flow and increases normal tissue blood flow. Age- and sex-matched athymic nude mice were injected with an MDA-MB-435 tumor cell line to the lateral thigh. When lesions reached 1 cm in size, laser Doppler analysis of tumor blood flow was performed (A, B). After obtaining baseline perfusion data, therapeutic agents were given through rectal bolus (DEA/NO 1 μl/g weight of 100-mM stock). Data sampling was then done every 2.5 minutes. Results represent the mean ± SD of five separate experiments. Representative images are presented. Age- and sex-matched Cr(Cnr) athymic<nu>fBf mice underwent laser Doppler analysis of normal hind limb perfusion (A, B). After obtaining baseline perfusion data, DEA/NO (1 μl/g weight of 100-mM stock) was given through rectal bolus. Data sampling was then done every 2.5 minutes. Results represent the mean ± SD of four separate animals. Representative images are presented. Scale bar, 10 mm.

responses to a greater extent in tumor explants from wild type mice to essentially match that of melanoma explants from TSP1 null mice (Figure 1*A*, *left panel*). Conversely, addition of exogenous TSP1 suppressed the outgrowth of the melanoma explants from the TSP1 null mice to match that of explants from wild type mice (Figure 1*A*, *right panel*).

MDA-MB-435 was previously considered to be a breast carcinoma cell line but was recently confirmed to be derived from the M14 melanoma cell line [43]. Parental MDA-MB-435 cells express very low levels of TSP1 [44] and form metastatic tumors with strong angiogenic potential when grown as xenografts in athymic mice [40]. Growth of the parental cells and TSP1-transfected clones as subcutaneous xenografts in Cr(Cnr) nude mice essentially reproduced our previously published growth curves after mammary fat pad injection (Figure 1*B*). TH26 express high levels of intact TSP1 that suppresses tumor growth, whereas TH50 cells overexpress a C-terminally truncated TSP1 that lacks this activity [40].

Consistent with their *in vivo* growth rates, tumor explants of these three clones showed markedly different vascular cell outgrowth in three-dimensional cultures. Maximum cell outgrowth occurred in explants of the parental cell line and TH50 clone with minimal enhancement by NO (Figure 1*C*). A control vector transfectant showed slightly less vascular outgrowth. In sharp contrast, the TH26 clone demonstrated no basal vascular cell response and decreased outgrowth after stimulation with exogenous NO (51.3 ± 4.3% less outgrowth compared to MDA-MB-435 explants). Immunohistochemical detection of endothelial cells by anti-CD31 staining of cytospins recovered from the outgrowths verified that overexpression of TSP1 in the TH26 explants inhibited endothelial cell outgrowth (Figure 1*D*). Thus, TSP1 expressed either in the tumor vasculature or by the tumor can limit vascular outgrowth in this tumor explant angiogenesis assay.

Coculture experiments corroborated these findings. Postconfluent monolayers of BAECs are known to spontaneously form sprouts and tubes in culture that express characteristic proangiogenic genes [45]. Quiescent confluent BAECs grown under Transwell chambers containing MDA-MB-435 cells exposed the BAECs to diffusible factors secreted by the tumor cells that significantly enhance sprouting and branching of the BAEC (Figure 1*E*, *center panel*). In contrast, BAEC exposed to factors released by the TSP1-expressing clone TH26 cells maintained their quiescent morphology (*right panel*), indicating that the level of TSP1 secreted by TH26 cells effectively

blocks the branching and sprouting response stimulated by proangiogenic factors released by this melanoma cell line.

Endogenous TSP1 in the Tumor Vasculature Does Not Limit NO-Driven Perfusion in B16F10 Melanoma Tumors

Wild type and TSP1 null mice bearing B16F10 tumors underwent BOLD MRI to assess acute changes in tumor perfusion induced by systemic NO treatment. Average-intensity analysis of the BOLD signal integrated over the indicated areas of interest (Figure 2, *A* and *B*) demonstrated the expected net increase in BOLD signal in normal tissue, with the increase being greater in the TSP1 null mice (Figure 2*C*). In contrast, the average BOLD signal decreased approximately 5% in the B16F10 tumors of both wild type and TSP1 null mice (Figure 2*C*). This decrease is consistent with decreased blood flow into the tumor due to a steal effect resulting from the peripheral vasodilation by the administered NO. Laser Doppler analysis of normal hind limb perfusion in C57BL/6 wild type and TSP1 null mice after an NO challenge confirmed the data obtained by BOLD MRI (Figure 2*D*). Increased blood flow was detected in TSP1 null limbs within 2.5 minutes after administering the NO donor, and increased flow relative to wild type limbs was maintained for the duration of measurement.

Further analysis of the BOLD MRI data selecting areas showing positive *versus* negative signals confirmed our previous finding in healthy mouse skeletal muscle that endogenous TSP1 limits the increased BOLD MRI signal in the normal tissue in response to NO

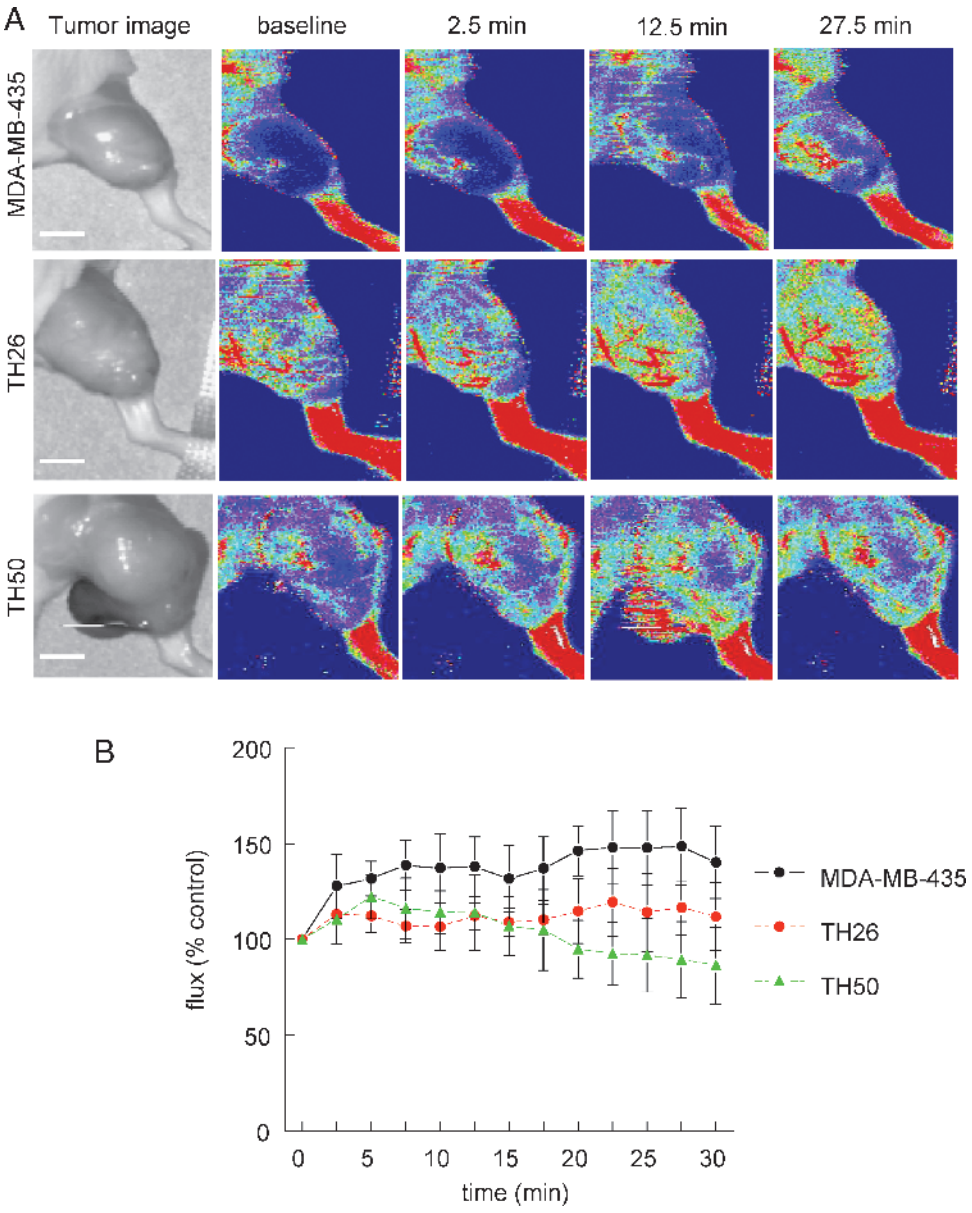

Figure 5. Thrombospondin 1 expression in MDA-MB-435 melanomas tempers vasoactive tumor blood flow responses to vasodilator or vasopressor challenge. Age- and sex-matched athymic nude mice were injected with equal numbers of either parental MDA-MB-435, clone TH26, or clone TH50 cells to the lateral thigh. When lesions reached 1 cm in size, laser Doppler analysis of tumor blood flow was performed. After obtaining baseline perfusion data, therapeutic agents were given [epinephrine, 0.002 μg/g weight through i.p. injection (A, B); DEA/NO, 1 μl/g weight through rectal bolus (C, D)]. Data sampling was then done every 2.5 minutes. Results represent the mean ± SD of five separate experiments. Representative images are presented. See Movie W2 for a real-time movie of tumor blood flow. Scale bar, 10 mm.

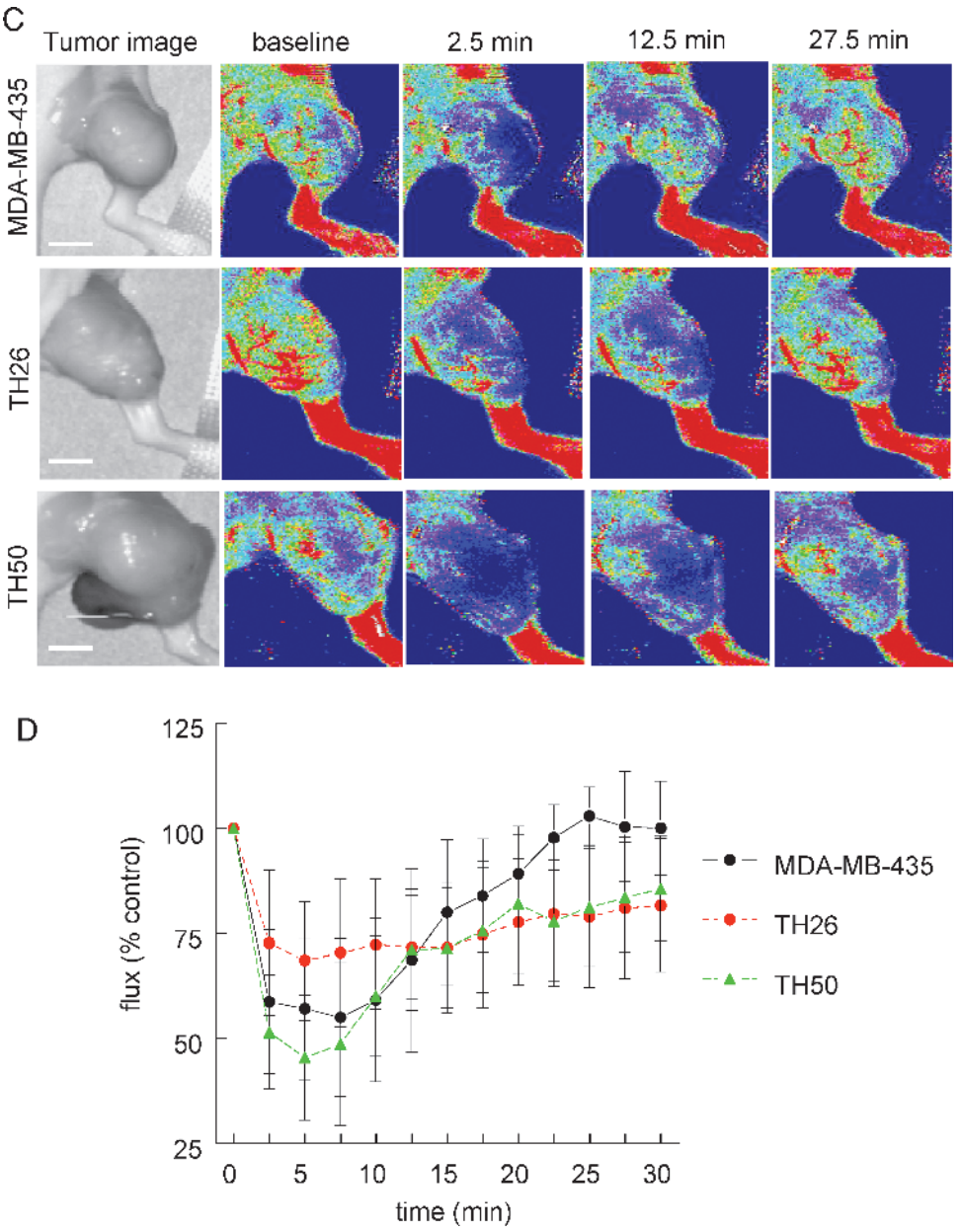

Figure 5. (*continued*)

challenge in areas with positive signal but did not influence those with negative response (Figure 3*A*). In the tumors, however, neither positive nor negative BOLD MRI signals differed between wild type and TSP1 null mice (Figure 3*B*). Thus, the *Thbs1* genotype of vascular cells recruited into these melanomas does not significantly influence their acute response to NO, and the net effect of a systemic NO challenge (Figure 2*C*) is to acutely decrease blood oxygen levels in the tumor secondary to increasing flow in normal peripheral tissue (Figure 2, *C* and *D*; see Movie W1 for a real-time movie of tumor blood flow).

Tumor TSP1 Limits NO-Stimulated Alterations in Tumor Blood Flow and Perfusion

Consistent with the results in C57BL/6 mice (Figures 2 and 3), normal vascular beds in contralateral hind limbs of the athymic mice demonstrated increased blood flow as determined by laser Doppler after a vasoactive challenge with exogenous NO (Figure 4, *A* and *B*).

To address whether overexpression TSP1 by the tumor can control tumor blood flow, athymic nude mice were injected with MDA-MB-435 tumor cells engineered to express variable amounts of TSP1. Parental MDA-MB-435 cells express very low levels of TSP1 [44]. On the basis of laser Doppler imaging, epinephrine moderately but rapidly increased blood flow in these tumors, which was sustained over 30 minutes (Figure 5, *A* and *B*). Relative to the parental tumors, tumors formed by the TSP1 overexpressing clone TH26 demonstrated attenuated changes in tumor perfusion after vasoactive challenge using epinephrine (Figure 5, *A* and *B*; see Movie W2 for a real-time movie of tumor blood flow). Epinephrine did not significantly increase blood flow in these tumors. The TH50 clone overexpresses a C-terminal truncated form of TSP1, lacking residues 1073 to 1152 of the mature protein and shown previously to not inhibit MDA-MB-435 tumor growth [40]. The epinephrine response of these tumors was also attenuated relative to the parental cells and returned to baseline by 30 minutes.

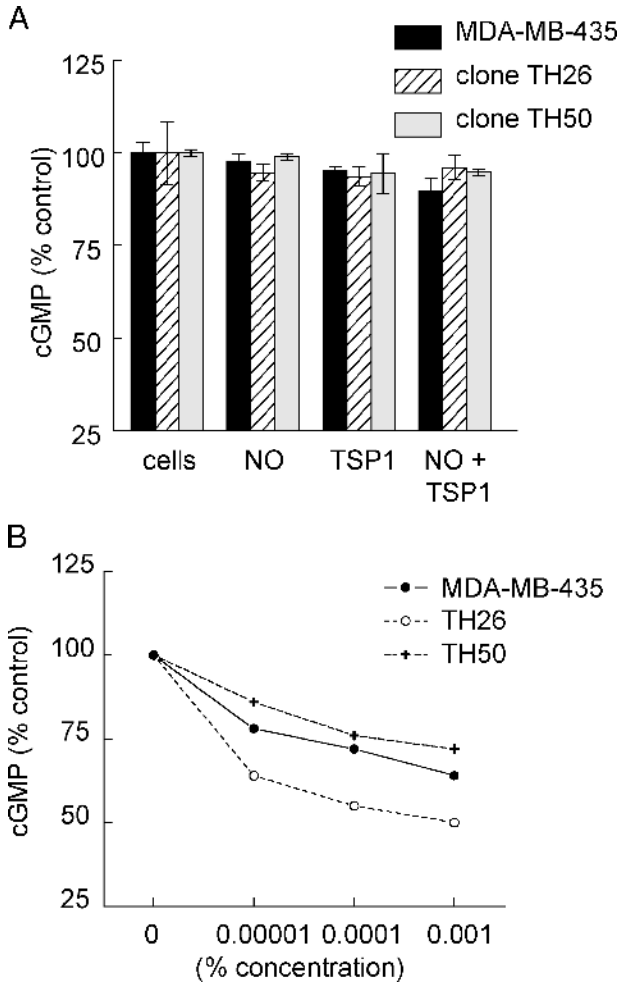

Figure 6. MDA-MB-435 melanoma cells do not demonstrate NO- or TSP1-sensitive cGMP signaling. MDA-MB-435, clone TH26, and clone TH50 tumor cells (2.5×10^4/well) were plated in RPMI and allowed to adhere for 12 hours. The next day, cells were incubated for 2.5 minutes in basal medium (lacking serum) ± DETA/NO (10 μM) ± TSP1 (2.2 nM), and cGMP levels were determined by immunoassay (A). Results represent the mean ± SD of three separate experiments. Porcine femoral artery VSMCs were plated (2.5×10^4/well) in 12-well plates in growth medium, weaned of serum over 48 hours, incubated in the indicated concentrations of tumor-conditioned medium (0.01–1% in basal smooth muscle medium + 0.1% BSA) for 15 minutes, and DEA/NO (10 μM) was added for 2.5 minutes. Cells were lysed and cGMP determined through ELISA (B). Results presented are representative of three separate experiments.

Conversely, administering NO to mice bearing parental MDA-MB-435 tumors resulted in a rapid 50% decrease in tumor blood flow over the first 10 minutes that returned toward baseline by 30 minutes (Figure 5, *C* and *D*). Thrombospondin 1-expressing TH26 tumors demonstrated less than half as much decrease in tumor perfusion after an NO challenge than that seen in parental MDA-MB-435 tumors with changes persisting over the 30 minutes measuring period. Because the C-terminal domain of TSP1 is recognized by the CD47 receptor that mediates its antagonism of NO signaling [36], we also examined NO responses in these tumors. Tumors formed by TH50 cells exhibited a similar response to NO as the parental MDA-MB-435 tumors. The immediate decrease in tumor perfusion returned to baseline by 30 minutes (Figure 5, *C* and *D*; see Movie W3 for a real-time movie of tumor blood flow). Therefore, this truncated TSP1 lacks the ability to functionally limit acute NO responses *in vivo*.

MDA-MB-435 Tumor Cells Lack NO–cGMP Signaling

A number of human tumors have been reported to have decreased levels of or lack TSP1 expression [46–49]. Although NO signaling stimulated by tumor-produced angiogenic factors under such conditions should be increased in vascular cells [15], it is not known whether NO and TSP1 can similarly regulate cGMP signaling in tumor cells. Analysis of parental MDA-MB-435 cells and the TH50 and TH26 clones demonstrated no significant change in cGMP levels after treatment with either exogenous NO or TSP1 (Figure 6*A*). Analysis of several additional cancer cell lines including B16F10 melanoma, PC3 prostate carcinoma, and SKOV3 ovarian carcinoma cells demonstrated a similar lack of NO-cGMP signaling (data not shown). Therefore, cGMP signaling responses to NO in these tumors are restricted to the tumor vasculature.

MDA-MB-435 Clone TH26–Conditioned Medium Limits NO-Driven cGMP Accumulation in VSMC

To assess the ability of the truncated TSP1 secreted by TH50 cells to regulate vascular cGMP signaling, porcine VSMCs were treated with conditioned medium from parental MDA-MB-435, TH26, and TH50 cells. cGMP was quantified after a challenge with 10 μM DEA/NO. Not surprisingly, the medium from the TSP1-overexpressing TH26 clone potently blocked an NO-driven cGMP flux (Figure 6*B*). Conditioned medium from the parental MDA-MB-435 cells was less effective at equivalent concentrations for suppressing NO-stimulated cGMP accumulation in VSMC. The residual inhibition in the parental cell–conditioned medium may be due to the low level of endogenous TSP1 expressed by these cells [44]. Medium obtained from the TH50 clone did not significantly abrogate an NO-driven flux in cGMP in VSMC relative to the parental cells, indicating that this C-terminally truncated TSP1 is a less effective inhibitor of NO/cGMP signaling.

Discussion

The use of NO and other vasoactive agents for controlling tumor blood flow remains controversial. Although some evidence indicates that NO does not acutely and directly alter tumor blood flow [2,5,50], others have reported a diminution of tumor blood flow after NO synthase inhibition *in vivo* [19,20,50–54]. Conversely, increased tumor blood flow has been noted with exogenous NO administration [17,51]. Some of these disparities may be attributed to variations in imaging modalities and techniques, vasoactive agents used, and the specific tumor models. We used two distinct and complementary noninvasive imaging modalities, BOLD MRI and laser Doppler, which are highly reproducible in both animals and people. Analysis of a syngeneic murine melanoma (B16F10) and a human xenograft melanoma (MDA-MB-435) demonstrate that NO does not show significant vasodilator activity for the tumor vasculature. Regardless of murine strain or tumor cell line studied, administration of exogenous NO resulted in a rapid decrease in tumor blood flow as documented by both BOLD MRI and laser Doppler. Decreased blood flow in the abnormal vascular network of the tumor was paralleled by a concurrent increase in blood flow in adjacent and distant normal vascular networks (Figures 2*C*, 3*A*, and 4, *A* and *B*), establishing that NO drives a redistribution of blood away from the tumor

vessels through active dilation of normal vascular networks through a steal effect. Conversely, constriction of peripheral vasculature using epinephrine acutely increased blood flow into these tumors, presumably by increasing the mean pressure in arteries supplying the tumor. Therefore, the tumor behaves in both cases as a passive resistance whose flow is inversely related to that in the host periphery.

The presence of TSP1 in the tumor vasculature and surrounding normal tissues of the host animal had minimal effects on acute regulation of tumor blood flow. In contrast, overexpression of TSP1 by the tumor cells significantly attenuated blood flow changes after NO treatment (Figure 5, *C* and *D*), supporting a role for TSP1 in modulating tumor blood flow responses. Intravenous treatment with the type 1 repeats of TSP1 was inferred to alter blood flow in pancreatic tumors [39]. Assessed by intravenous injection of fluorescein-labeled dextran and histologic analysis of excised tumors, treated animals had decreased total vessel area and less fluorescence signal in CD31-positive vessels. Although suggesting a decrease in vessel filling and blood flow, these findings may represent primarily a loss of perfused vessels rather than a change in flow, which was not directly assessed. The type 1 repeats can block NO signaling in vascular cells through CD36 [15,55], but our previous studies in ischemic injury models indicate that CD36 signaling does not significantly contribute to acute regulation of blood flow [38]. Thus, the antitumor activity of TSP1-based drugs targeting CD36 may occur exclusively through inhibiting angiogenesis rather than flow, the latter being controlled through CD47.

At the cellular level, vascular cells are the major target for this acute activity of NO in tumors because most tumor cells do not demonstrate NO-driven cyclic nucleotide signaling. MDA-MB-435 cells and clones from the same parent did not demonstrate an accumulation of intracellular cGMP after treatment with NO. This lack of response is not unique to MDA-MB-435 cells. Several other common tumor cell lines including B16F10, PC3, and SKOV3 cells failed to demonstrate a cGMP flux after NO treatment (data not shown). Tumor blood vessels have also been found incapable of producing NO in response to acetylcholine [56]. Thus, tumors generally lack NO-responsive cGMP signaling.

Consistent with our data, increased tumor blood flow has been found in animal models after challenge with one [3,57,58] or more vasoconstrictors [59] alone or in combination with β-blockers such as propranolol [60]. The same response has been confirmed in patients [32,61]. However, the increased tumor perfusion induced by systemic treatment with vasoconstrictors was relatively brief. Prolonged increases in tumor blood flow could only be achieved through continuous infusion of the vasoconstrictor [3]. In a xenograft soft tissue tumor model, we found moderate enhancement of tumor blood flow after a single i.p. dose of epinephrine. As with NO, blood flow changes to epinephrine were tempered in tumors that overexpress TSP1. In all cases, tumor blood flow tended to return to baseline within 30 minutes. Although similar agents can modify tumor blood flow in people, their use may be limited by increases in heart rate and blood pressure [61].

Tumor blood flow, therefore, is a passive response to alterations in flow and resistance in the nontumor vascular networks and system of the host both regionally and centrally. If vascular resistance beyond the tumor decreases, as with administration of exogenous NO, blood rapidly drains from the tumor. Alternatively, increasing peripheral vascular resistance in normal vascular networks with a centrally acting hypertensive agent redistributes blood into the tumor vasculature. Acutely, the tumor vasculature is resistant to vasoactive challenge and registers no direct response.

Acknowledgments

The authors thank Larry Keefer and Joseph Saavedra (National Cancer Institute, Frederick, MD) for providing NO donors.

References

[1] Zhu X, Wu S, Dahut WL, and Parikh CR (2007). Risks of proteinuria and hypertension with bevacizumab, an antibody against vascular endothelial growth factor: systematic review and meta-analysis. *Am J Kidney Dis* **49**, 186–193.

[2] Zlotecki RA, Baxter LT, Boucher Y, and Jain RK (1995). Pharmacologic modification of tumor blood flow and interstitial fluid pressure in a human tumor xenograft: network analysis and mechanistic interpretation. *Microvasc Res* **50**, 429–443.

[3] Shankar A, Loizidou M, Burnstock G, and Taylor I (1999). Noradrenaline improves the tumour to normal blood flow ratio and drug delivery in a model of liver metastases. *Br J Surg* **86**, 453–457.

[4] McDonald DM and Baluk P (2005). Imaging of angiogenesis in inflamed airways and tumors: newly formed blood vessels are not alike and may be wildly abnormal: Parker B. Francis lecture. *Chest* **128**, 602S–608S.

[5] Peterson HI (1991). Modification of tumour blood flow—a review. *Int J Radiat Biol* **60**, 201–210.

[6] Mollica F, Jain RK, and Netti PA (2003). A model for temporal heterogeneities of tumor blood flow. *Microvasc Res* **65**, 56–60.

[7] Fukumura D, Yuan F, Endo M, and Jain RK (1997). Role of nitric oxide in tumor microcirculation. Blood flow, vascular permeability, and leukocyte–endothelial interactions. *Am J Pathol* **150**, 713–725.

[8] Kumagai Y, Toi M, and Inoue H (2002). Dynamism of tumour vasculature in the early phase of cancer progression: outcomes from oesophageal cancer research. *Lancet Oncol* **3**, 604–610.

[9] Jain RK (2001). Delivery of molecular and cellular medicine to solid tumors. *Adv Drug Deliv Rev* **46**, 149–168.

[10] Munn LL (2003). Aberrant vascular architecture in tumors and its importance in drug-based therapies. *Drug Discov Today* **8**, 396–403.

[11] Feldmann HJ, Molls M, and Vaupel P (1999). Blood flow and oxygenation status of human tumors. Clinical investigations. *Strahlenther Onkol* **175**, 1–9.

[12] Tozer GM, Kanthou C, and Baguley BC (2005). Disrupting tumour blood vessels. *Nat Rev Cancer* **5**, 423–435.

[13] Hinnen P and Eskens FA (2007). Vascular disrupting agents in clinical development. *Br J Cancer* **96**, 1159–1165.

[14] Ignarro LJ (2002). Nitric oxide as a unique signaling molecule in the vascular system: a historical overview. *J Physiol Pharmacol* **53**, 503–514.

[15] Isenberg JS, Ridnour LA, Perruccio EM, Espey MG, Wink DA, and Roberts DD (2005). Thrombospondin-1 inhibits endothelial cell responses to nitric oxide in a cGMP-dependent manner. *Proc Natl Acad Sci USA* **102**, 13141–13146.

[16] Ridnour LA, Thomas DD, Donzelli S, Espey MG, Roberts DD, Wink DA, and Isenberg JS (2006). The biphasic nature of nitric oxide responses in tumor biology. *Antioxid Redox Signal* **8**, 1329–1337.

[17] Fukumura D and Jain RK (1998). Role of nitric oxide in angiogenesis and microcirculation in tumors. *Cancer Metastasis Rev* **17**, 77–89.

[18] Tozer GM, Prise VE, Wilson J, Cemazar M, Shan S, Dewhirst MW, Barber PR, Vojnovic B, and Chaplin DJ (2001). Mechanisms associated with tumor vascular shut-down induced by combretastatin A-4 phosphate: intravital microscopy and measurement of vascular permeability. *Cancer Res* **61**, 6413–6422.

[19] Meyer RE, Shan S, DeAngelo J, Dodge RK, Bonaventura J, Ong ET, and Dewhirst MW (1995). Nitric oxide synthase inhibition irreversibly decreases perfusion in the R3230Ac rat mammary adenocarcinoma. *Br J Cancer* **71**, 1169–1174.

[20] Tozer GM, Prise VE, and Chaplin DJ (1997). Inhibition of nitric oxide synthase induces a selective reduction in tumor blood flow that is reversible with L-arginine. *Cancer Res* **57**, 948–955.

[21] Yuan F, Salehi HA, Boucher Y, Vasthare US, Tuma RF, and Jain RK (1994). Vascular permeability and microcirculation of gliomas and mammary carcinomas transplanted in rat and mouse cranial windows. *Cancer Res* **54**, 4564–4568.

[22] Brizel DM, Klitzman B, Cook JM, Edwards J, Rosner G, and Dewhirst MW (1993). A comparison of tumor and normal tissue microvascular hematocrits and red cell fluxes in a rat window chamber model. *Int J Radiat Oncol Biol Phys* **25**, 269–276.

[23] de Wilt JH, Manusama ER, van Etten B, van Tiel ST, Jorna AS, Seynhaeve AL, ten Hagen TL, and Eggermont AM (2000). Nitric oxide synthase inhibition results in synergistic anti-tumour activity with melphalan and tumour necrosis factor alpha-based isolated limb perfusions. *Br J Cancer* **83**, 1176–1182.

[24] Jordan BF, Misson P, Demeure R, Baudelet C, Beghein N, and Gallez B (2000). Changes in tumor oxygenation/perfusion induced by the no donor, isosorbide dinitrate, in comparison with carbogen: monitoring by EPR and MRI. *Int J Radiat Oncol Biol Phys* **48**, 565–570.

[25] Van Buren G II, Camp ER, Yang AD, Gray MJ, Fan F, Somcio R, and Ellis LM (2006). The role of nitric oxide in mediating tumour blood flow. *Expert Opin Ther Targets* **10**, 689–701.

[26] Chaplin DJ, Hill SA, Bell KM, and Tozer GM (1998). Modification of tumor blood flow: current status and future directions. *Semin Radiat Oncol* **8**, 151–163.

[27] Lala PK and Orucevic A (1998). Role of nitric oxide in tumor progression: lessons from experimental tumors. *Cancer Metastasis Rev* **17**, 91–106.

[28] Shan SQ, Rosner GL, Braun RD, Hahn J, Pearce C, and Dewhirst MW (1997). Effects of diethylamine/nitric oxide on blood perfusion and oxygenation in the R3230Ac mammary carcinoma. *Br J Cancer* **76**, 429–437.

[29] Shinoda J and Whittle IR (2001). Nitric oxide and glioma: a target for novel therapy? *Br J Neurosurg* **15**, 213–220.

[30] Ng QS, Goh V, Milner J, Stratford MR, Folkes LK, Tozer GM, Saunders MI, and Hoskin PJ (2007). Effect of nitric-oxide synthesis on tumour blood volume and vascular activity: a phase I study. *Lancet Oncol* **8**, 111–118.

[31] Roberts DD, Isenberg JS, Ridnour LA, and Wink DA (2007). Nitric oxide and its gatekeeper thrombospondin-1 in tumor angiogenesis. *Clin Cancer Res* **13**, 795–798.

[32] Andrews JC, Walker-Andrews SC, Juni JE, Warber S, and Ensminger WD (1989). Modulation of liver tumor blood flow with hepatic arterial epinephrine: a SPECT study. *Radiology* **173**, 645–647.

[33] Good DJ, Polverini PJ, Rastinejad F, Le Beau MM, Lemons RS, Frazier WA, and Bouck NP (1990). A tumor suppressor-dependent inhibitor of angiogenesis is immunologically and functionally indistinguishable from a fragment of thrombospondin. *Proc Natl Acad Sci USA* **87**, 6624–6628.

[34] Taraboletti G, Roberts D, Liotta LA, and Giavazzi R (1990). Platelet thrombospondin modulates endothelial cell adhesion, motility, and growth: a potential angiogenesis regulatory factor. *J Cell Biol* **111**, 765–772.

[35] Lawler J and Detmar M (2004). Tumor progression: the effects of thrombospondin-1 and -2. *Int J Biochem Cell Biol* **36**, 1038–1045.

[36] Isenberg JS, Ridnour LA, Dimitry J, Frazier WA, Wink DA, and Roberts DD (2006). CD47 is necessary for inhibition of nitric oxide–stimulated vascular cell responses by thrombospondin-1. *J Biol Chem* **281**, 26069–26080.

[37] Isenberg JS, Hyodo F, Matsumoto K, Romeo MJ, Abu-Asab M, Tsokos M, Kuppusamy P, Wink DA, Krishna MC, and Roberts DD (2007). Thrombospondin-1 limits ischemic tissue survival by inhibiting nitric oxide–mediated vascular smooth muscle relaxation. *Blood* **109**, 1945–1952.

[38] Isenberg JS, Romeo MJ, Abu-Asab M, Tsokos M, Oldenborg A, Pappan L, Wink DA, Frazier WA, and Roberts DD (2007). Increasing survival of ischemic tissue by targeting CD47. *Circ Res* **100**, 712–720.

[39] Zhang X, Connolly C, Duquette M, Lawler J, and Parangi S (2007). Continuous administration of the three thrombospondin-1 type 1 repeats recombinant protein improves the potency of therapy in an orthotopic human pancreatic cancer model. *Cancer Lett* **247**, 143–149.

[40] Weinstat-Saslow DL, Zabrenetzky VS, VanHoutte K, Frazier WA, Roberts DD, and Steeg PS (1994). Transfection of thrombospondin 1 complementary DNA into a human breast carcinoma cell line reduces primary tumor growth, metastatic potential, and angiogenesis. *Cancer Res* **54**, 6504–6511.

[41] Lawler J, Miao WM, Duquette M, Bouck N, Bronson RT, and Hynes RO (2001). Thrombospondin-1 gene expression affects survival and tumor spectrum of p53-deficient mice. *Am J Pathol* **159**, 1949–1956.

[42] Isenberg JS, Jia Y, Field L, Ridnour LA, Sparatore A, Del Soldato P, Sowers AL, Yeh GC, Moody TW, Wink DA, et al. (2007). Modulation of angiogenesis by dithiolethione-modified NSAIDs and valproic acid. *Br J Pharmacol* **151**, 63–72.

[43] Rae JM, Creighton CJ, Meck JM, Haddad BR, and Johnson MD (2007). MDA-MB-435 cells are derived from M14 melanoma cells—a loss for breast cancer, but a boon for melanoma research. *Breast Cancer Res Treat* **104**, 13–19.

[44] Zabrenetzky V, Harris CC, Steeg PS, and Roberts DD (1994). Expression of the extracellular matrix molecule thrombospondin inversely correlates with malignant progression in melanoma, lung and breast carcinoma cell lines. *Int J Cancer* **59**, 191–195.

[45] Fouser L, Iruela-Arispe L, Bornstein P, and Sage EH (1991). Transcriptional activity of the alpha 1(I)-collagen promoter is correlated with the formation of capillary-like structures by endothelial cells *in vitro*. *J Biol Chem* **266**, 18345–18351.

[46] Michaud M and Poyet P (1994). Control of the expression of thrombospondin 1 in human breast cancer cell lines. *Anticancer Res* **14**, 1127–1131.

[47] Ordonez JL, Paraoan L, Hiscott P, Gray D, Garcia-Finana M, Grierson I, and Damato B (2005). Differential expression of angioregulatory matricellular proteins in posterior uveal melanoma. *Melanoma Res* **15**, 495–502.

[48] Bastian M, Steiner M, and Schuff-Werner P (2005). Expression of thrombospondin-1 in prostate-derived cell lines. *Int J Mol Med* **15**, 49–56.

[49] Iddings DM, Koda EA, Grewal SS, Parker R, Saha S, and Bilchik A (2007). Association of angiogenesis markers with lymph node metastasis in early colorectal cancer. *Arch Surg* **142**, 738–744; discussion 744–745.

[50] Natori Y, Moriguchi M, Fujiwara S, Takeshita I, Fukui M, Iwaki T, and Kanaide H (1992). Effects of L-NMMA and L-NNA on the selective ATP-induced enhancement of intratumoral blood flow. *J Cereb Blood Flow Metab* **12**, 120–127.

[51] Swaroop GR, Malcolm GP, Kelly PA, Ritchie I, and Whittle IR (1998). Effects of nitric oxide modulation on tumour blood flow and microvascular permeability in C6 glioma. *Neuroreport* **9**, 2577–2581.

[52] Tozer GM, Prise VE, Motterlini R, Poole BA, Wilson J, and Chaplin DJ (1998). The comparative effects of the NOS inhibitor, N^{ω}-nitro-L-arginine, and the haemoxygenase inhibitor, zinc protoporphyrin IX, on tumour blood flow. *Int J Radiat Oncol Biol Phys* **42**, 849–853.

[53] Andrade SP, Hart IR, and Piper PJ (1992). Inhibitors of nitric oxide synthase selectively reduce flow in tumor-associated neovasculature. *Br J Pharmacol* **107**, 1092–1095.

[54] Whittle IR, Collins F, Kelly PA, Ritchie I, and Ironside JW (1996). Nitric oxide synthase is expressed in experimental malignant glioma and influences tumour blood flow. *Acta Neurochir (Wien)* **138**, 870–875; discussion 875–876.

[55] Isenberg JS, Jia Y, Fukuyama J, Switzer CH, Wink DA, and Roberts DD (2007). Thrombospondin-1 inhibits nitric oxide signaling via CD36 by inhibiting myristic acid uptake. *J Biol Chem* **282**, 15404–15415.

[56] Tozer GM, Prise VE, Bell KM, Dennis MF, Stratford MR, and Chaplin DJ (1996). Reduced capacity of tumour blood vessels to produce endothelium-derived relaxing factor: significance for blood flow modification. *Br J Cancer* **74**, 1955–1960.

[57] Hemingway DM, Chang D, Cooke TG, and Jenkins SA (1991). The effects of vasopressin infusion on hepatic haemodynamics in an experimental model of liver metastases. *Br J Cancer* **64**, 212–214.

[58] Ackerman NB, Jacobs R, Bloom ND, and Poon TT (1988). Increased capillary flow in intrahepatic tumors due to alpha-adrenergic effects of catecholamines. *Cancer* **61**, 1550–1554.

[59] Hemingway DM, Cooke TG, Chang D, Grime SJ, and Jenkins SA (1991). The effects of intra-arterial vasoconstrictors on the distribution of a radiolabelled low molecular weight marker in an experimental model of liver tumour. *Br J Cancer* **63**, 495–498.

[60] Burton MA and Gray BN (1987). Redistribution of blood flow in experimental hepatic tumours with noradrenaline and propranolol. *Br J Cancer* **56**, 585–588.

[61] Hemingway DM, Angerson WJ, Anderson JH, Goldberg JA, McArdle CS, and Cooke TG (1992). Monitoring blood flow to colorectal liver metastases using laser Doppler flowmetry: the effect of angiotensin II. *Br J Cancer* **66**, 958–960.

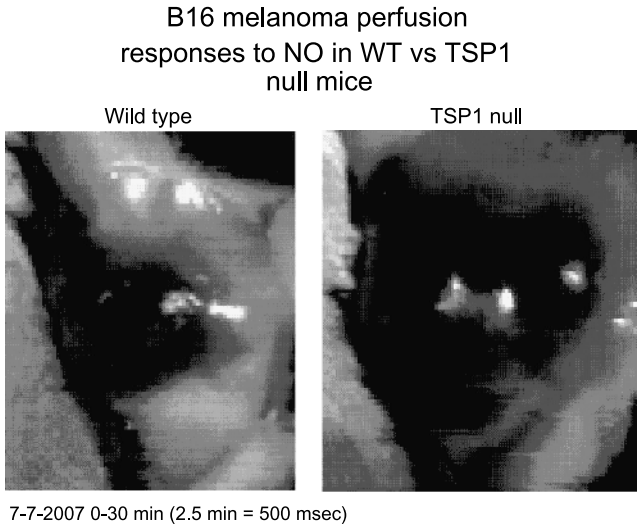

Movie W1. Syngeneic B16 melanoma perfusion responses to NO in wild type *versus* TSP1 null mice. Each movie shows an initial light image followed by a pretreatment Doppler image and a time lapse movie (500 milliseconds = 2.5 minutes) of Doppler scans taken over 30 min after administration of DEA/NO as a rectal bolus.

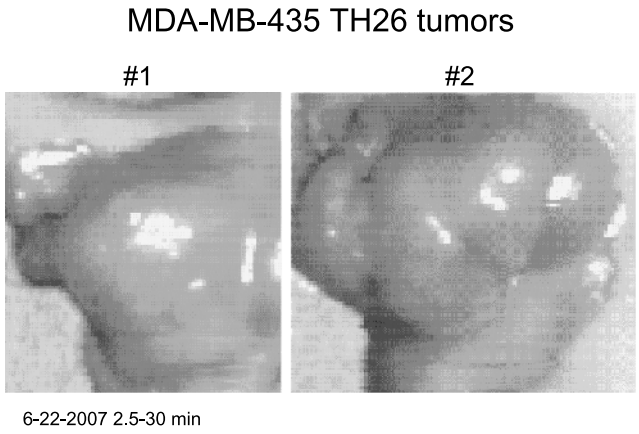

Movie W2. Perfusion responses to NO in a M14 (MDA-MB-435) human melanoma xenograft overexpressing full-length thrombospondin-1 (clone TH26). Time lapse movies (500 milliseconds = 2.5 minutes) of Doppler scans taken over 30 min after administration of DEA/NO as a rectal bolus.

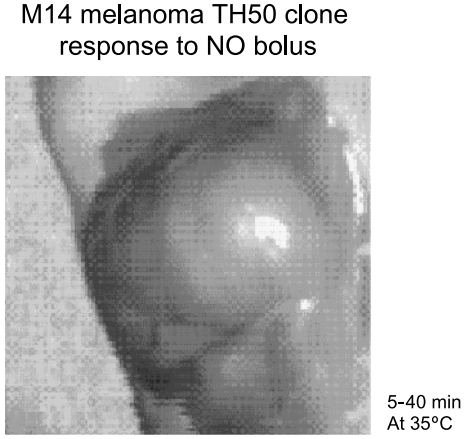

Movie W3. Perfusion responses to NO in a M14 (MDA-MB-435) human melanoma xenograft overexpressing C-terminal–truncated thrombospondin-1 (clone TH50). Time lapse movie (500 milliseconds = 5 minutes) of Doppler scans taken over 40 min after administration of DEA/NO as a rectal bolus.